

THEORETICAL STUDY OF $4p^5nl n'l'SJ$ STATES OF Sr ION EXCITED BY ELECTRON IMPACT ON Sr ATOM

A. Kupliauskienė*

Institute of Theoretical Physics and Astronomy, Vilnius University, Saulėtekio 3, 10257 Vilnius, Lithuania

Email: tfai@tfai.vu.lt

Received 10 January 2018; revised 15 March 2018; accepted 21 June 2018

Calculations of energy levels and electron-impact excitation cross sections of the Auger autoionizing states $4p^5nl n'l'$ ($nl = 4d, 5s, 5p$; $n'l' = 4d, 5s, 5p, 5d, 6s, 6p, 6d, 7s, 7p$) of Sr ion were performed. A large-scale configuration interaction method on the basis of the solutions of Dirac–Fock–Slater equations was used. The cross sections of electron-impact simultaneous ionization and excitation, and Auger decay of the electron-impact excited states of Sr atom to the $4p$ -core excited autoionizing states of Sr ion were calculated for the first time and used to estimate the intensity of ejected electron lines. Tentative identification of the Auger electron lines of Sr ion registered in a number of experiments is presented.

Keywords: electronic structure of atoms and molecules, theory, autoionization, atomic excitation and ionization

PACS: 31.15.-p, 32.80.Zb, 34.80.Dp

1. Introduction

The highest filled p subshell excitation in photoionization of alkaline earth atoms Mg, Ca and Sr has been investigated for many years and reviewed in detail by C. Banahan et al. [1]. The dipole allowed transitions populate core-excited states of alkaline earth ions with the total angular momenta $J = 1/2, 3/2$. Electron-impact excitation and ionization processes are more powerful tools allowing to obtain states with all possible values of the total angular momentum J resulting in registration of more lines in the Auger decay spectrum [2–10]. Theoretical investigation of those spectra is complicated as the correlation effects play a significant role both for creation ways and decay channels of states. Therefore, for the classification of states, more than one set

of quantum numbers can be assigned due to strong configuration mixing.

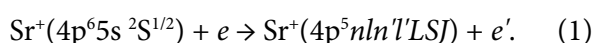
Investigation of Sr atoms is important for many fields including medicine as their structure is similar to that of Ca, thus Sr can substitute Ca in living organisms. For example, Sr was inserted into core-excited pellets and used for cancer diagnosis and treatment [11]. The Auger electrons from the core-excited states, both $np^5n'l'n''l''$ ($n = 3, 4, 5$) of the alkaline earth ions and $np^5nl n'l'n''l''$ of the alkaline earth atoms Ca, Sr and Ba, were registered in the same experiments of the interaction of Ca, Sr and Ba atoms with electrons [2–9]. Schmitz et al. [3] studied the excitation and ionization of $3p$ electrons in Ca and $4p$ electrons in Sr, and dominant mechanisms leading to Auger and autoionization effects at 2 keV incident electron energy. The measurements were carried out at 90° with respect to the direction of projectile electrons. They registered 34 ejected electron lines of Sr and assigned 2 of them to Sr^+ . A similar investigation was carried out at much lower incident electron

* The community of Lithuanian physicists experienced a loss on 18 May 2018 when Alicija Kupliauskienė suddenly died. Her papers were often published in the Lithuanian Journal of Physics, she was the laureate of the 2013 year Lithuanian Science Prize.

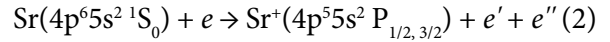
energies of 23.5, 38, 50, 75, 150 and 500 eV in [4]. 20 lines were attributed to Sr^+ . The measurements were carried out at 75° with respect to the direction of projectile electrons. 10 lines measured in [7] at 200 eV electron impact were assigned to Sr^+ as well. The electrostatic energy analyzer recorded electrons emitted at 90° with respect to the primary electron beam. In [3, 4, 7] experiments, the identification of ejected electron lines of Sr^+ was not performed except the states $4p^55s^2\ ^2P_{1/2, 3/2}$. The measurements at the ‘magic’ angle 54.7° were performed in [6] for 45, 80, 100 and 1500 eV energies of incident electrons. A small number of the measured lines were identified, i.e. 27 lines were measured and 13 lines of them were attributed to Sr^+ .

Theoretical calculations of the 4p-core excited states of Sr^+ are not numerous. Mansfield and Newsom [5] have performed calculations by using the Cowan code [15] including configuration mixing (CI) and relativistic corrections, and proposed the identification of 18 lines of Sr^+ registered in [4]. The following configurations were used: $4p^5(5s^2 + 4d5s + 4d^2 + 5p^2)$. 19 levels which belong to these configurations were presented. The values of energy levels for the $4p^54d(^1\text{P})5s\ ^2P$ terms relative to the ground state were calculated in [16] by using both Hartree–Fock and multiconfiguration Hartree–Fock approximations [17]. The same configurations as in [5] were included to construct the basis set and take into account correlation effects. CI semi-relativistic calculations by using the Cowan suite of codes [15] were performed in the LSJ and jjJ coupling schemes of angular momenta [1] for the transitions from the states of configurations $4p^65s$ and $4p^64d$ to $4p^55s(nd, ms)$, $4p^54d(ns, md)$ and $4p^55p^2$. The Slater–Condon parameters were reduced to optimize the calculated transition energy with the experiment. The calculated energies were also used for the identification of Sr^+ lines in the region between 26.0 and 37.4 eV measured in photoabsorption experiments [1]. The identification of 7 lines of Sr^+ was performed in [6] by using the excitation energies calculated in the single configuration Hartree–Fock approximation.

The autoionizing states of Sr ions can be populated by several processes. One of them is the excitation of Sr^+ by electron (e) impact:

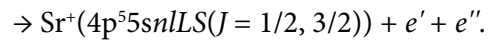


But the core-excited states of Sr^+ can also be populated in other processes of electrostatic interaction of Sr atoms with electrons. The direct ionization (DI) of the 4p shell



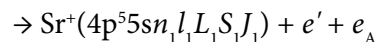
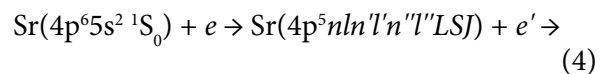
is the most probable process. These two lines should be most intensive in the electron-impact excited Auger electron spectrum as the ionization cross section is about 27 and 17 Mb for $4p^55s^2\ ^2P_{3/2}$ and $^2P_{1/2}$, respectively, in the case of 38 eV impacting electron energy used by White et al. [4] compared to the excitation cross sections for the states of the $4p^5nln'l'LSJ$ Sr atom which are not larger than 8 Mb.

A simultaneous ionization and excitation (SIE) process very effective in light alkali atoms [18] can also populate the states of Sr ion:



Our calculations show that these cross sections are less than 30 Mb. The contribution of the SIE process for Ba atoms was estimated by Nienhaus et al. [12].

The autoionization process of electron-impact excited Sr atoms



can also be an effective way to populate the 4p-core excited states of Sr ions. It can be called the excitation-autoionization (EA) process [12, 13]. The ejection of Auger lines of Ba ions in the double autoionization in Ba atoms was confirmed experimentally by J.P. Connerade et al. [14]. In (1)–(3), e , e' and e'' indicate the impacting, scattered and emitted electrons, respectively, and e_A is the Auger electron.

The purpose of the present work was to perform *ab initio* calculations of the excitation energies, excitation and ionization cross sections for the $4p^5nln'l'LSJ$ ($nl = 4d, 5s, 5p$; $n'l' = 4d, 5s, 5p, 5d, 6s, 6p, 6d, 7s, 7p$) states of Sr ion by using a large scale CI approximation in the basis of relativistic Dirac–Fock–Slater [19] radial orbitals. Estimation

of the cross sections of direct electron-impact ionization, SIE and EA processes and the decay of the electron-impact excited states of Sr atom to the 4p-core excited states of Sr ion, and application of their values for the identification of the Auger lines of Sr ion registered in experiments [3, 4, 7] on Sr atoms were also a task of the present work.

2. Method of calculations

The calculations of energies, electron-impact excitation and ionization cross sections were performed by using the Flexible Atomic Code (FAC) [19]. It uses a modified Dirac–Fock–Slater potential that includes an approximate treatment of the exchange part. The radial orbitals for the construction of basis state wave functions were derived from a modified self-consistent Dirac–Fock–Slater iteration on a fictitious mean configuration with fractional occupation numbers representing the average electron cloud of all configurations included in the calculation. Since the local potential was optimized only for singly excited configurations, to reduce the errors on total state energies the following correction procedure was applied. Before the potential for the mean configuration with fractional occupation numbers was calculated, the optimized potential and corresponding average energy for each configuration was obtained. Then, the average energy for each configuration was calculated with the potential optimized for the mean configuration with fractional occupation numbers. The difference of two average energies was applied as a correction to the states within each configuration after the Hamiltonian was diagonalized.

The calculations of the values of excitation energies and electron-impact excitation cross sections of Sr⁺ were carried out separately from the calculations of DI, SIE and EA cross sections. For Sr⁺, the optimization of a local central potential, which includes the approximated exchange part, the singly excited configurations 4p⁶nl (nl = 6–11s, 5–11p, 4–11d, 4–11f, 5–8g) were used. The correlation effects were taken into account by adding the 4p-core excited 4p⁵nl'n''l'' (nl = 5s, 5p, 4d, 4f; n'l' = 5–10s, 5–10p, 4–10d, 4–10f; 5–7g), 4p⁵6s² and 4p⁵5d5f configurations. The total number of states was 5 486.

To estimate the population of Sr⁺ 4p-core excited states, the calculations of DI (2) and SIE (3) cross sections, and the autoionization probabilities of the 4p-core highly excited states of Sr atom were performed by using the FAC computer code [19] in the common basis set of configurations joining both Sr and Sr⁺. For the optimization of the local central potential, the ground and singly excited 4p⁶5snl (nl = 5–10s; 5–10p; 4–7f; 5–7g) configurations of Sr were used. To take into account correlation effects in Sr, the ground and singly excited 4p⁶5snl (nl = 4–10d, 5–10p, 6–10s, 4–7f, 5–7g) and the 4p-core excited configurations 4p⁵nl'n''l'' (nl = 5s, 4d, 5p, 4f; n'l' = 5s, 5p, 6s, 7s, 4d, 5d, 6d, 4f, 5f; n''l'' = 5d, 6d, 7d, 6s, 7s, 8s, 6p, 7p, 8p, 5f, 6f, 7f, 5g) were used. The following configurations of Sr⁺ 4p⁶nl (nl = 5s, 6s, 5p, 6p, 4d, 5d, 4f), 4p⁵5s², 4p⁵4d², 4p⁵4d5s, 4p⁵5s5p, 4p⁵4d5p, 4p⁵5s6s, 4p⁵5p², and 4p⁵4d5d were added to the basis set of Sr configuration. The total number of both odd and even states included in the calculation for Sr and Sr⁺ was 30 101. The same basis set was used to calculate electron-impact excitation cross sections, and to describe the final state in the ionization of Sr atoms. The autoionization probabilities of Sr atom were calculated for the transitions to the 4p⁶nl (nl = 5s, 6s, 5p, 6p, 4d, 5d, 4f), 4p⁵5s², 4p⁵4d², 4p⁵4d5s, 4p⁵5s5p, 4p⁵4d5p, 4p⁵5s6s, 4p⁵5p² and 4p⁵4d5d configurations of Sr⁺ to include energetically allowed decay channels for the levels with energy greater than 26.92 eV [10].

The energy levels calculated with the FAC code were described by the quantum numbers *jjJ* of the relativistic coupling scheme of angular momenta. Since the non-relativistic *LSJ* coupling scheme is more familiar to experimenters and is more popular for classifying the experimental spectrum, the expansion coefficients obtained in the *jjJ* coupling scheme were transformed to the *LSJ* coupling scheme [20].

As the accuracy of calculations is less than the difference of energies between some highly excited autoionizing levels, for the identification of measured spectra the additional information was involved, i.e. the intensity of ejected electron lines was estimated. The intensity $I(\alpha LSJ, J_e)$ of a line, ejected after the interaction of an atom or ion with an electron without taking into account the asymmetry of the angular distribution of emitted Auger electrons, can be written as follows [21, 22]:

$$I(\alpha LSJ, J_f) \sim \frac{\sigma(\alpha LSJ)}{4\pi} B(\alpha LSJ, J_f). \quad (5)$$

In (5), $B(\alpha LSJ, J_f)$ is the Auger decay branching ratio, αLSJ indicates the configuration and other quantum numbers, L and S are total orbital and spin angular momenta, J and J_f are the total angular momenta of the state of an ion and the final state of a doubly ionized atom, respectively. $\sigma(\alpha LSJ)$ can be the total excitation cross section of an atom excited by electrons or photons from the ground state to the autoionizing state αLSJ . $\sigma(\alpha LSJ)$ can also be the cross section of DI (2) and SIE (3) from the inner shell of an atom by electrons or the cross section of autoionization from the core-excited levels of Sr atoms (4). In (5), the cross section is used instead of the excitation rate as a beam of electrons with the fixed velocity is used in electron-impact experiments. There is no distribution of electrons over velocities that is characteristic of plasma.

The Auger electron branching ratio is defined as

$$B(\alpha LSJ, J_f) = \frac{A^a(\alpha LSJ, J_f)}{\sum_i A_i^r(\alpha LSJ) + \sum_j A_j^a(\alpha LSJ, J_f)}. \quad (6)$$

Our calculations have shown that the radiative transition probabilities $A_i^r(\alpha LSJ)$ from the initial state αLSJ to all final states i are much smaller than the autoionization probabilities $A_j^a(\alpha LSJ, J_f)$. Therefore, it can be assumed that

$$B(\alpha LSJ, J_f) \simeq \frac{A^a(\alpha LSJ, J_f)}{\sum_j A_j^a(\alpha LSJ, J_f)}. \quad (7)$$

Moreover, in the case of core excited states of alkali atoms, only one Auger decay channel is possible [23, 24], therefore $B(\alpha LSJ, J_f) = 1$.

The cross section for the process (4) can be written as

$$\sigma(\alpha LSJ) = \sum_i \sigma(0 \rightarrow i) \frac{A^a(i \rightarrow \alpha LSJ)}{\sum_k A^a(i \rightarrow k)}. \quad (8)$$

Here $\sigma(0 \rightarrow i)$ is the electron-impact excitation cross section of Sr atom from the ground state 0 to the autoionizing state i , $A^a(i \rightarrow \alpha LSJ)$ is the autoionization probability from the autoionizing state i of Sr to the core-excited state αLSJ of Sr^+ , $A^a(i \rightarrow k)$ is the Auger decay probabilities of Sr atom to all possible final ground, singly excited as well as core

excited states of Sr^+ . The radiative decay channel is ignored as its probabilities are much smaller than the corresponding autoionization ones mentioned above. The contribution of radiative cascades to populate lower levels from higher ones can be expected to be small as the values of autoionization probabilities by more than four orders of magnitude exceed the values of radiative transition probabilities. For the calculation of cross sections (8), a computer program was created.

3. Results and discussion

The values of excitation energies (E , eV), the largest expansion coefficient c used for the assignment of quantum numbers, the excitation cross sections (σ , 10^{-18} cm²) for 38 and 500 eV of incident electrons, the ejected electron energies (E_{ej} , eV), the SIE cross section σ_{SIE} (3) (10^{-18} cm²) and the EA cross section σ_{EA} (4) (10^{-18} cm²) at 38 eV electron-impact energies for the $4p^5nl(L_1S_1)n'l'SJ$ states of Sr^+ are presented in Table 1. More lines in the ejected electron spectrum can be expected if the excitation, SIE and EA cross sections are large, therefore the states for which at least one of those cross sections is larger than 0.4 Mb are included in Table 1. In the case of ionization of Sr to $4p^55s^2\ ^2P_{1/2, 3/2}$ of Sr^+ , the SIE coincides with the DI cross section.

The choice of the coupling scheme of angular momenta was made by comparing the expansion coefficients in LSJ and jjJ coupling schemes. The analysis has shown that the LSJ coupling scheme was more suitable than the jjJ one. For the levels presented in Table 1, the expansion coefficient in the LSJ coupling scheme used for the classification was larger than the one in the jjJ coupling scheme. Several exceptions were noticed in the case of the levels with energy 22.750, 23.417, 24.290, 26.954, 27.884, 29.501, 30.938, 31.130 and 31.161 eV. But for the levels with 22.826, 23.417, 26.954, 27.884 and 29.501 eV, the expansion coefficient c was much larger in the jjJ coupling scheme than in the LSJ one. For these levels, they were 0.56 and 0.25, 0.58 and 0.41, 0.44 and 0.29, 0.39 and 0.29, 0.63 and 0.43 for the jjJ and LSJ coupling schemes, respectively. The values of expansion coefficients c presented in Table 1 indicate that the LSJ coupling scheme fits well for the largest part of calculated levels. Such conclusion can be expected as the nuclear charge of Sr is not large,

Table 1. Excitation energies (E , eV), the largest expansion coefficient c , the excitation cross sections (σ , 10^{-18} cm 2) for 38 and 500 eV of incident electrons, the ejected electron energies (E_{ej} , eV), the SIE cross section (σ_{SIE} (2), 10^{-18} cm 2) and the EA cross section (σ_{EA} (3), 10^{-18} cm 2) for Sr $^+$ $4p^5nl(L_1S_1)n'l'LSJ$ states.

E	c	State	σ_{38}	σ_{500}	E_{ej}	σ_{SIE}	σ_{EA}
21.217	0.97	$4d(^3P)5s\ ^4P_{1/2}$	2.81	0.004	10.187	0.01	3.10
21.380	0.97	$4d(^3P)5s\ ^4P_{3/2}$	5.52	0.02	10.350	0.24	6.69
21.661	0.95	$4d(^3P)5s\ ^4P_{5/2}$	7.70	0.004	10.631		3.23
21.957	0.85	$4d(^3P)5s\ ^2P_{1/2}$	2.24	0.06	10.927	1.64	4.01
22.020	0.60	$4d(^3P)5s\ ^2P_{3/2}$	4.55	0.23	10.990	23.21	6.24
22.054	0.98	$4d(^3F)5s\ ^4F_{9/2}$	4.41		11.024		0.86
22.112	0.86	$4d(^3F)5s\ ^4D_{1/2}$	0.77	0.06	11.082	0.59	3.96
22.130	0.78	$4d(^3F)5s\ ^4D_{3/2}$	1.05	0.20	11.100	8.08	5.74
22.213	0.91	$4d(^3F)5s\ ^4F_{7/2}$	2.95	0.02	11.183		5.42
22.285	0.71	$4d(^3F)5s\ ^4D_{7/2}$	0.85	0.01	11.255		3.42
22.443	0.91	$4d(^3F)5s\ ^4F_{5/2}$	2.64	0.04	11.413		5.79
22.718	0.91	$4d(^3F)5s\ ^4F_{3/2}$	1.63		11.688	4.08	10.04
22.750	0.25	$4d(^1F)5s\ ^2F_{7/2}$	3.26	0.06	11.720		2.32
22.826*	0.41	$4d(^3F)5s\ ^2F_{5/2}$	1.15		11.796		2.68
22.896	0.77	$5s^2\ ^2P_{3/2}$	4.48	1.14	11.866	26.99	20.74
23.286	0.82	$4d(^3P)5s\ ^4P_{5/2}$	0.45		12.256		3.67
23.413	0.52	$4d(^3F)5s\ ^2F_{5/2}$	0.6	0.10	12.383		4.47
23.413	0.47	$4d(^1D)5s\ ^2D_{3/2}$	1.76	0.22	12.383	1.15	3.90
23.417*	0.29	$4d(^3D)5s\ ^4D_{5/2}$	1.82	0.11	12.387	3.32	
23.516	0.75	$4d(^3D)5s\ ^4D_{7/2}$	2.84	0.29	12.486		2.75
23.874	0.55	$4d(^1F)5s\ ^2F_{5/2}$	1.38	0.07	12.844		1.73
23.880	0.90	$5s^2\ ^2P_{1/2}$	0.69	0.93	12.850	17.16	8.35
23.999	0.72	$5s(^3P)5p\ ^4S_{3/2}$	1.21		12.969		0.80
24.052	0.46	$4d(^1D)5s\ ^2D_{5/2}$	0.80		13.022		1.66
24.073	0.87	$4d(^3D)5s\ ^4D_{3/2}$	1.84	0.20	13.043	0.02	6.34
24.098	0.96	$4d(^3D)5s\ ^4D_{1/2}$	1.18	0.11	13.068	4.21	3.10
24.144	0.51	$4d(^1G)5s\ ^2F_{7/2}$	0.73	0.05	12.114		1.44
24.230*	0.39	$4d(^3F)5s\ ^4G_{5/2}$	1.02	0.07	13.200		3.15
24.249	0.85	$4d(^1D)5s\ ^2P_{1/2}$	0.23	0.08	13.221	5.51	6.37
24.302	0.86	$4d(^1D)5s\ ^2D_{3/2}$	1.42	0.11	13.272	1.11	2.53
24.331	0.64	$5s(^3P)5p\ ^4D_{7/2}$	0.42		13.301		0.55
24.354	0.64	$4d(^1D)5s\ ^2D_{5/2}$	1.22	0.06	13.324		4.13
24.418	0.63	$4d(^1F)5s\ ^2F_{7/2}$	2.62	0.29	13.388		1.66
24.477	0.54	$4d(^3D)5s\ ^2D_{3/2}$	1.07	0.24	13.447	0.33	1.96
24.500	0.63	$4d(^3D)5s\ ^2D_{7/2}$	1.80	0.15	13.470		2.37
24.771	0.75	$4d(^1D)5s\ ^2F_{7/2}$	0.84	0.11	13.741		2.35

Table 1 (continued)

E	c	State	σ_{38}	σ_{500}	E_{ej}	σ_{SIE}	σ_{EA}
24.924	0.75	$4d^2(^1D) ^2D_{5/2}$	0.82		13.894		2.59
25.177*	0.48	$4d(^1P)5p ^2S_{1/2}$	1.10	0.09	14.147		0.19
25.359	0.60	$5s(^1P)5p ^2D_{5/2}$	0.43	0.01	14.329	0.02	0.64
25.372*	0.40	$4d(^1D)5p ^2D_{3/2}$	0.74	0.10	14.342		0.80
25.427	0.67	$4d(^3P)5p ^4D_{7/2}$	0.41		14.397		0.07
25.500	0.61	$4d(^3P) ^4D_{3/2}$	0.42	0.05	14.470	0.06	4.95
25.521	0.63	$5s(^3P)5p ^2D_{5/2}$	0.56	0.04	14.491	0.64	
25.575	0.54	$5s(^3P)5p ^4P_{3/2}$	0.52	0.07	14.545		0.56
25.827	0.72	$4d^2(^1D) ^2F_{5/2}$	0.56	0.04	14.797		0.55
26.149	0.67	$5s(^3P)5p ^4P_{1/2}$	1.49	0.12	15.119		0.10
26.441	0.72	$5s(^3P)5p ^2D_{3/2}$	0.54	0.04	15.411		0.14
26.617	0.52	$4d(^3D)5p ^4P_{5/2}$	0.93	0.16	15.587		0.23
26.633	0.61	$5s(^3P)5p ^2P_{3/2}$	0.42		15.603		0.10
26.780	0.84	$4d^2(^1S) ^2P_{3/2}$	2.19	0.65	15.750	0.09	
26.954	0.36	$5s(^3P)5p ^2P_{1/2}$	0.85	0.05	15.924		0.09
27.174	0.58	$5s(^3P)5p ^2P_{1/2}$	3.09	0.28	16.144		0.04
27.535	0.85	$4d^2(^1S) ^2P_{1/2}$	6.60	2.06	16.505	0.57	0.10
27.864	0.74	$4d(^3D)5p ^4P_{1/2}$	1.64	0.19	16.834		0.06
27.884*	0.29	$4d(^1P)5p ^2P_{1/2}$	7.62	0.82	16.854		0.04
27.919	0.91	$4d(^3P)6s ^4P_{1/2}$	0.56	0.17	16.889	0.05	
27.978	0.67	$4d(^1P)5s ^2P_{1/2}$	15.12	4.69	16.948	0.04	
27.988	0.76	$4d(^1P)5s ^2P_{3/2}$	44.13	13.77	16.958		
28.066	0.87	$4d(^3P)6s ^4P_{3/2}$	5.62	1.75	17.036	0.01	
28.173	0.91	$4d(^3P)6s ^2P_{1/2}$	4.04	1.18	17.143	0.03	
28.292	0.46	$4d(^3P)5d ^4D_{3/2}$	0.70	0.19	17.262		0.02
28.406	0.75	$4d(^3P)6s ^2P_{3/2}$	4.10	1.17	17.376	0.28	
28.605	0.37	$4d(^3F)5d ^2P_{3/2}$	0.69	0.23	17.575	0.08	0.24
28.630	0.50	$4d(^3P)5d ^2P_{3/2}$	0.49	0.15	17.600	0.04	0.22
28.866	0.59	$4d(^3P)5d ^4P_{3/2}$	0.64	0.20	17.836	0.05	0.09
28.976	0.47	$4d(^3P)5d ^4D_{3/2}$	2.27	0.70	17.946		0.10
29.066	0.47	$4d(^1D)5d ^2D_{3/2}$	2.11	0.61	18.036	0.02	0.08
29.115	0.59	$5p^2(^3P) ^4P_{3/2}$	1.64	0.54	18.085	0.06	0.04
29.182	0.71	$4d(^3P)5d ^2P_{1/2}$	5.45	1.68	18.152		0.06
29.427	0.71	$5s(^3P)6s ^4P_{3/2}$	1.32	0.52	18.397	1.15	0.01
29.501	0.43	$5p^2(^1D) ^2P_{1/2}$	1.59	0.44	18.471		0.01
29.524	0.51	$5p^2(^1D) ^2P_{3/2}$	6.16	2.03	18.494	0.06	0.02
29.577	0.73	$5s(^1P)6s ^2P_{1/2}$	3.00	1.21	18.547	0.39	0.01
29.830	0.75	$5s(^3P)5d ^4P_{1/2}$	0.49	0.11	18.800	0.03	

Table 1 (continued)

E	c	State	σ_{38}	σ_{500}	E_{ej}	σ_{SIE}	σ_{EA}
29.849	0.60	5s(³ P)5d ⁴ P _{3/2}	0.45	0.08	18.819	0.02	
30.015	0.67	4d(³ F)5d ⁴ D _{5/2}	0.48	0.14	18.985		
30.160	0.47	5s(¹ P)5d ² P _{1/2}	0.62	0.15	19.130	0.27	
30.216	0.51	4d(³ F)5d ⁴ P _{1/2}	0.40	0.11	19.186		
30.481	0.87	5s(³ P)6s ⁴ P _{1/2}	0.55	0.19	19.451	0.03	0.01
30.567	0.49	5s(³ P)5d ² P _{1/2}	0.52	0.14	19.537	0.27	
30.589	0.61	4d(³ P)7s ² P _{3/2}	0.70	0.28	19.559		
30.614	0.58	4d(¹ D)7s ² D _{3/2}	0.64	0.20	19.584		
30.620	0.51	4d(³ D)7s ² D _{3/2}	0.62	0.21	19.590	0.02	
30.731	0.74	5p ² (³ P) ² S _{1/2}	1.31	0.40	19.701		0.01
30.748	0.56	5p ² (³ P) ⁴ S _{3/2}	0.64	0.19	19.718	0.03	0.01
30.771	0.44	5s(³ P)5d ⁴ D _{1/2}	2.74	0.83	19.741	0.03	
30.842	0.69	4d(³ P)5d ² S _{1/2}	0.57	0.17	19.812	0.27	
30.862	0.46	5s(¹ P)5d ² P _{3/2}	4.88	1.50	19.908	0.39	
30.938	0.37	4d(³ D)5d ⁴ S _{3/2}	0.42	0.12	19.908		
30.989	0.52	5s(³ P)6p ² S _{1/2}	2.26	0.25	19.959		
30.991	0.35	4d(³ P)7s ² P _{3/2}	0.59	0.20	19.961		
30.999	0.71	4d(³ D)5d ² F _{3/2}	0.46	0.12	19.969	0.01	
31.115	0.63	4d(³ P)7p ² S _{1/2}	0.53	0.07	20.085		
31.130	0.34	5s(¹ P)6d ² P _{3/2}	2.25	0.64	20.100		
31.161	0.45	4d(³ F)6d ² D _{3/2}	1.43	0.43	20.131	0.01	

* The second or third expansion coefficient was used for the classification of the level.

and the effective nuclear charge felt by other electrons is small. Therefore, the *LSJ* coupling scheme of angular momenta of the $4p^5nl n' l' LSJ$ states is used for the classification. The quantum numbers were assigned to the levels by using a term with the largest expansion coefficient. In the cases when two levels are described by the largest expansion coefficient of the same term, one of them was classified by using the quantum numbers of the larger coefficient, and the other level obtained the quantum numbers of the second or even the third term. These levels are marked with a star in Table 1. The SIE cross section is not equal to zero only for the states of $4p^54d5s$, $4p^55s^2$, $4p^55s6s$ and $4p^54d^2$ configurations of Sr^+ with $J = 1/2, 3/2$ and is larger for the low levels. Its values rapidly decrease with increasing the principal quantum number n of excited electrons.

The comparison of the excitation energies calculated in [1] with those of the present work is complicated as different orders of 5s and 4d subshells are used in the coupling of angular momenta. In the present work, the order is $4p^54d5s$, while $4p^55s4d$ is used in [1]. The cases of $4p^54d(^1P)5s^2P_{3/2}$ and $4p^54d(^3P)6s^2P_{1/2}$ are an exception, but these lines are not seen in the electron-impact spectrum. Therefore, they were not included in Table 2 for comparison. But the comparison of energies calculated in [1] and the present work is possible in the case of the lowest levels $4p^54d5s$ *LSJ* by using the theoretical energies presented in Table 1 [1]. For the state $(^3P)^4P_{1/2}$, the energies are 21.137 and 21.217 eV in [1] and the present work, respectively. For the second state $(^3P)^4P_{3/2}$, they are 21.275 [1] and 21.380 eV. In the case of higher levels, the agreement is worse, e.g. 21.702 [1] and

21.957 eV for $(^3P)^2P_{1/2}$, 21.820 [1] and 22.020 eV for $(^3P)^2P_{3/2}$, and 22.465 [1] and 22.718 eV for $(^3F)^4F_{3/2}$. A large disagreement can be noticed in the case of $5s(^1P)6s^2P_{1/2}$, for which the calculated energy is 30.27 eV in [1], the experiment value is 29.33 [1] and 29.58 eV in the present work.

The comparison of the excitation energies calculated in the present work and by Mansfield and Newsom [5], and the calculated ejected electron energies with the experimental data [3, 4, 7] are

presented in Table 2. The suggested identifications from [5] based on the present calculations are also included in Table 2. The excitation energies calculated in [5] are lower by about 0.12 eV than those calculated in the present work. The agreement between the calculated energies and the assignment of quantum numbers is very good for the first 6 lowest levels, while the agreement between higher levels is worse. The assignment of quantum numbers to the 9 lowest levels and some higher

Table 2. Comparison of the calculated excitation (E , eV) and ejected (E_{ej} , eV) electron energies with the excitation energies calculated by Mansfield (E [5]) and the measured ejected electron energies (E_{ej} [4], E_{ej} [7], E_{ej} [3]) for the $4p^5nl n'l'SJ$ states of Sr^+ .

State	E	E_{ej}	State [5]	E [5]	E_{ej} [4]	E_{ej} [7]	E_{ej} [3]
$4d(^3P)5s\ ^4P_{1/2}$	21.217	10.19	$4d5s\ ^4P_{1/2}$	21.098	10.20	10.18	
$4d(^3P)5s\ ^4P_{3/2}$	21.380	10.35	$4d5s\ ^4P_{3/2}$	21.247	10.34	10.31	10.35
$4d(^3P)5s\ ^4P_{5/2}$	21.661	10.63	$4d5s\ ^4P_{5/2}$	21.527	10.61	10.59	10.62
$4d(^3P)5s\ ^2P_{1/2}$	21.957	10.93	$4d(^3P)5s\ ^2P_{1/2}$	21.814	10.80		
$4d(^3P)5s\ ^2P_{3/2}$	22.020	10.99	$4d(^3P)5s\ ^2P_{3/2}$	21.898	10.89	10.89	10.91
$4d^2(^3F)\ ^4D_{3/2}$	22.130	11.10	$4d^2(^3F)\ ^4D_{3/2}$	22.018	11.03	11.04	11.05
$4d(^3F)5s\ ^4F_{7/2}$	22.213	11.18			11.18	11.21	
$4d^2(^3F)\ ^4F_{5/2}$	22.443	11.41			11.27	11.30	
$4d(^3F)5s\ ^4F_{3/2}$	22.718	11.69			11.65	11.59	11.51
$5s^2\ ^2P_{3/2}$	22.896	11.87	$5s^2\ ^2P_{3/2}$	22.535	11.46	11.46	11.48
$4d(^1F)5s\ ^2F_{5/2}$	22.826	11.80			11.83	11.80	
$4d^2(^3F)\ ^2F_{5/2}$	23.413	12.38			11.91		
$4d^2(^1D)\ ^2D_{3/2}$	23.413	12.38	$4d^2(^1D)\ ^2D_{3/2}$	23.119	12.06	12.03	
$4d(^3D)5s\ ^2D_{5/2}$	23.417	12.39	$4d^2\ ^4P_{3/2}$	23.115	12.13		
$4d(^3D)5s\ ^4D_{7/2}$	23.516	12.49	$4d^2\ ^4P_{1/2}$	23.317	12.21		
$5s^2\ ^2P_{1/2}$	23.880	12.85	$5s^2\ ^2P_{1/2}$	23.517	12.43	12.40	12.45
$4d(^1F)5s\ ^2F_{5/2}$	23.874	12.84			12.64		12.65
$4d(^3D)5s\ ^4D_{1/2}$	24.098	13.07	$4d5s\ ^4D_{1/2}$	23.669	12.70		12.71
$4d^2(^1D)\ ^2P_{1/2}$	24.249	13.22	$4d^2(^3P)\ ^2P_{3/2}$	23.832	12.92		
$4d^2(^1D)\ ^2D_{3/2}$	24.302	13.27	$4d^2(^1D)\ ^2P_{1/2}$	23.834	12.97		12.99
$4d^2(^1D)\ ^2D_{5/2}$	24.924	13.89			13.63		
$4d^2(^3P)\ ^4D_{3/2}$	25.500	14.47	$5p^2\ ^4S_{3/2}$	24.995	14.00	14.00	
$5s(^3P)5p\ ^4P_{3/2}$	25.575	14.55	$4d^2(^1S)\ ^2P_{3/2}$	26.202	14.82		
$5s(^1P)5p\ ^2S_{1/2}$	26.954	15.92	$4d^2(^1S)\ ^2P_{1/2}$	26.984	15.57	15.56	
$4d(^3P)5d\ ^4P_{3/2}$	28.866	17.84			17.57		
$5s(^3P)6s\ ^4P_{3/2}$	29.427	18.40	$5p^2(^1S)\ ^2P_{3/2}$	31.672	18.52		
$5s(^1P)6s\ ^2P_{1/2}$	29.577	18.55	$5p^2(^1S)\ ^2P_{1/2}$	32.812	18.26		

levels of the calculated spectrum [5] is the same as in the present work. For 9 higher levels, different quantum numbers from [5] are assigned. The reason for the difference can be explained by a different number of interacting configurations used in [5] and the present work. In [5], the configurations $4p^55s^2$, $4p^54d5s$, $4p^54d^2$ and $4p^55p^2$ were used to take into account the correlation effects and for classification. A larger number of used configurations led to the decrease of expansion coefficients which redistribute among more configurations. Therefore, different states had the largest expansion coefficient compared to those obtained in [5]. Moreover, it is worth to point out that the levels with 31.672 and 32.812 eV energy [5] cannot be used for the identification of the line the ejected electron energy of which is 18.35 eV as stated in [5], referring to the private communication with the authors of [4]. The reason for the difference can be caused by usage of the calculated intensities as an additional criterion for the calculated energies for the identification of lines in the present work.

The comparison of the calculated electron-impact and the sum of SIE and EA cross sections shows that the latter ones are larger for the largest part of the levels presented in Table 1 up to 26 eV energy of ejected electrons. The values of SIE and EA cross sections decrease with increasing energies of core-excited states. For other configurations, they are small, therefore the probability to populate their levels via the EA process is negligible.

For comparison of the calculated excitation energies with the energies of ejected electron lines in the experimental spectrum, identification of the ejected electron lines should be performed. The sum of DI, SIE and EA cross sections was used for this purpose as the intensity of lines is proportional to the probability of population of the level from which the line is emitted. EA cross sections are larger for the states of $4p^54d5s$, $4p^55s^2$, $4p^55s5p$ and $4p^54d^2$ configurations. The most intensive lines are 4, 5 and 9 in [4], 15, 19 and 24 in [7], and 3, 5 and 7 in [3]. The quantum numbers $4p^54d(^3P)5s^2P_{3/2}$, $4p^55s^2P_{3/2}$ and $4p^55s^2P_{1/2}$ can be assigned to them, respectively, as their intensities correlate very well with the sum of calculated cross sections for all impacting electron energies used in experiments [3, 4, 7]. The same assignment of lines 4, 5 and 6 measured in [4] was performed by Mansfield and Newsom [5]

as well. In the present work, the assignments for other lines were also performed by taking into account the correlation between the intensity of the ejected line and the sum of DI, SIE and EA cross sections. It is very important to ensure this correlation as the accuracy of the calculated excitation energies in the present work decreases while this energy increases. The next more intensive lines are 1, 2, 3, 18 and 20 at 500 eV impacting electrons and 31 at both 38 and 500 eV impacting electrons in the experimental spectrum [4]. Lines 1, 2, 3, 18 and 20 [4] can be identified as $4d(^3P)5s^4P_{1/2}$, $4d(^3P)5s^4P_{3/2}$, $4d(^3P)5s^4P_{5/2}$, $5s^2P_{1/2}$ and $4d(^3D)5s^4D_{3/2}$, as their theoretical cross sections are 3.11, 6.93, 3.23, 25.51 and 7.38 Mb, respectively, in a good agreement with the experimental intensities [4]. Line 10 is blended by line 9 [4]. It can be identified as $4d(^3F)5s^4F_{3/2}$. Its cross section 14.12 Mb is smaller compared with the cross section 42.73 Mb of line 9 [4]. The line with energy of 10.93 eV (10.80 eV [4]) is very close to line 4 [4], but it was resolved in a subsequent re-examination of the data (see [4, 5]). The intensities of lines 5, 7 and 8 in [4] correlate very well with the sum of SIE and EA cross sections presented in Table 1, i.e. they are 13.74, 5.42 and 5.79 Mb, respectively. The same correlation was observed for experimental lines 11–16 [4] which were identified as $4d(^1F)5s^2F_{5/2}$, $4d^2(^3F)^2F_{5/2}$, $4d^2(^1D)^2D_{3/2}$ and $4d(^3D)5s^2D_{5/2}$. Their cross sections are 2.68, 5.05, 3.22 and 2.75 Mb. The intensities of lines with the energy of ejected electrons 12.64 (19), 19.92 (23), 12.97 (22) and 13.63 eV (23) in [4] correlate well with the cross sections of $4d(^1F)5s^2D_{7/2}$ (1.73 Mb), $4d^2(^1D)^2P_{1/2}$ (11.88 Mb), $4d^2(^1D)^2D_{3/2}$ (3.64 Mb) and $4d^2(^1D)^2D_{5/2}$ (2.59 Mb), respectively. The calculated cross sections are much smaller for the levels starting from the level with 25.575 eV energy compared to the previous ones. The largest cross section of 1.16 Mb is for the state $4s(^3P)6s^4P_{3/2}$. It can be used for the assignment of quantum numbers for line 70 [4]. The lines included into Table 2 remain most intensive for all energies of impacting electrons used in the experiments [3, 4, 7].

4. Conclusions

Energy levels and electron-impact excitation cross sections of the autoionizing states $4p^5nl^n'l'$ ($nl = 4d$,

5s, 5p; $n'l' = 4d, 5s, 5p, 5d, 6s, 6p, 6d, 7s, 7p$) of Sr ion were calculated for the first time by using a large scale CI method in the bases of the solutions of Dirac–Fock–Slater equations. The cross sections of SIE and Auger decay of the electron-impact excited states of Sr atom to the 4p-core excited autoionizing states of Sr^+ were estimated for the 38 eV energy of impacting electrons on Sr atoms for the first time as well. A good correlation between the calculated sum of SIE and EA, and single electron ionization cross sections from the 4p subshell with the intensity of measured ejected electron lines of Sr^+ enabled us to perform the assignment of quantum numbers for all registered lines in the experiments of the interaction of Sr atom with electrons. The values of the ejected electron energies calculated in the present work and registered experimentally agreed very well only for the lowest levels, therefore the estimation of intensity served as the main tool used for the tentative identification. The calculations have shown that the intensities of Auger electron lines from the core-excited states of Sr^+ produced in SIE and EA processes are larger than the intensities of the same lines produced by electron impact in the case of low-lying states.

Acknowledgements

The author wishes to thank Dr. O. Zatsarinny of the Physics Department of Drake University for the transformation of expansion coefficients from the jjj to LSJ coupling scheme of angular momenta.

References

- [1] C. Banahan, J.T. Costello, D. Kilbane, and P. van Kampen, 4p-inner-shell and double-excitation spectrum of Sr II, *Phys. Rev. A* **79**(2), 022509 (2009), <https://doi.org/10.1103/physreva.79.022509>
- [2] D. Rassi and K.J. Ross, The ejected-electron spectrum of barium vapour autoionizing and Auger levels excited by 20–500 eV electrons, *J. Phys. B* **13**(23), 4683–4694 (1980), <https://doi.org/10.1088/0022-3700/13/23/024>
- [3] W. Schmitz, B. Breuckmann, and W. Mehlhorn, Low-energy electron spectra of atomic Ca and Sr excited by 2 keV electrons, *J. Phys. B* **9**(16), L493–L497 (1976), <https://doi.org/10.1088/0022-3700/9/16/007>
- [4] M.D. White, D. Rassi, and K.J. Ross, The ejected electron spectrum of strontium vapour autoionizing and Auger levels excited by 23.5 and 500 eV electrons, *J. Phys. B* **12**(2), 315–323 (1979), <https://doi.org/10.1088/0022-3700/12/2/020>
- [5] M.W.D. Mansfield and G.H. Newsom, The Sr I absorption spectrum in the vacuum ultraviolet: excitation of the 4p-subshell, *Proc. R. Soc. London A* **377**, 431–448 (1981), <https://doi.org/10.1098/rspa.1981.0134>
- [6] A.A. Borovik, I.S. Aleksakhin, V.F. Bratsev, and A.V. Kupliauskiene, Excitation and electron decay of the autoionizing states of the rare earth atoms: Strontium, *Opt. Spektrosk.* **53**(6), 976–980 (1982) [in Russian].
- [7] S.M. Kazakov and O.V. Khristoforov, Electron spectra from autoionizing states of strontium and calcium excited by low- and intermediate-energy electrons, *Sov. Phys. JETP* **61**(4), 656–664 (1985).
- [8] V. Hrytsko, G. Kerevičius, A. Kupliauskienė, and A. Borovik, The 5p autoionization spectra of Ba atoms excited by electron impact: identification of lines, *J. Phys. B* **49**, 145201 (2016), <https://doi.org/10.1088/0953-4075/49/14/145201>
- [9] A. Borovik, V. Vakula, and A. Kupliauskienė, The 4p⁶-core excited autoionizing states of strontium: classification and excitation dynamics, *Lith. J. Phys.* **47**(2), 129–135 (2007), <https://doi.org/10.3952/lithjphys.47203>
- [10] A. Kupliauskienė, G. Kerevičius, V. Borovik, I. Shafranyosh, and A. Borovik, The energy structure and decay channels of the 4p⁶ shell excited states in Sr, *J. Phys. B* **50**, 225201 (2017), <https://doi.org/10.1088/1361-6455/aa90df>
- [11] S.H. Tersigni, *Core-excited Nanoparticles and Methods of Their Use in the Diagnosis and Treatment of Disease*, Patent US8197471 B1, WO212112547A1 (2012).
- [12] J. Nienhaus, O.I. Zatsarinny, and W. Mehlhorn, Experimental and theoretical Auger and autoionization spectra for electron-impact on laser-excited Ba atom, *Phys. Essays* **13**(2–3), 307–324 (2000), <https://doi.org/10.4006/1.3028825>
- [13] A. Borovik, V. Roman, and A. Kupliauskienė, The 4p⁶ autoionization cross section of Rb at-

- oms excited by low-energy electron impact, *J. Phys. B* **45**(4), 045204 (2012), <https://doi.org/10.1088/0953-4075/45/4/045204>
- [14] J.P. Connerade, S.J. Rose, and I.P. Grant, Two-step autoionization and double ionization anomaly in Ba I, *J. Phys. B* **13**(2), L53–L55 (1979), <https://doi.org/10.1088/0022-3700/12/2/004>
- [15] R.D. Cowan, *The Theory of Atomic Structure and Spectra* (University of California Press, Berkeley, CA, 1981).
- [16] J.E. Hansen, The structure of the autoionizing p^5ds configurations in Ma II, Ca II, Sr II and Ba II and interpretation of electron impact cross sections in these ions, *J. Phys. B* **8**(17), 2759–2770 (1975), <https://doi.org/10.1088/0022-3700/8/17/007>
- [17] C. Froese Fischer, General Hatree-Fock program, *Comput. Phys. Commun.* **43**(3), 355–365 (1987), [https://doi.org/10.1016/0010-4655\(87\)90053-1](https://doi.org/10.1016/0010-4655(87)90053-1)
- [18] A. Kupliauskienė, On the application of relaxed-orbital and sudden perturbation approximations for photoionization of atoms, *J. Phys. B* **34**, 345–361 (2001), <https://doi.org/10.1088/0953-4075/34/3/312>
- [19] M.F. Gu, The flexible atomic code, *Can. J. Phys.* **86**(5), 675–689 (2008), <https://doi.org/10.1139/p07-197>
- [20] O. Zatsarinny (2016) [private communication].
- [21] A. Kupliauskienė, A general expression for the excitation cross-section of polarized atoms by polarized electrons, *Phys. Scripta* **75**(4), 524–530 (2007), <https://doi.org/10.1088/0031-8949/75/4/026>
- [22] A. Kupliauskienė and V. Tutlys, Properties of Auger electrons following excitation of polarized atoms by polarized electrons, *Nucl. Instrum. Methods B* **267**(2), 263265 (2009), <https://doi.org/10.1016/j.nimb.2008.10.039>
- [23] G. Kerevičius and A. Kupliauskienė, Classification of the $5p^5nl'n''LSJ$ energy levels of Cs excited by 30 eV electrons, *Lith. J. Phys.* **55**(2), 84 (2015), <https://doi.org/10.3952/physics.v55i2.3098>
- [24] S. Kour and R. Srivastava, Excitation of the lowest autoionizing $np^5(n+1)s^2P_{3/2,1/2}$ states of Na ($n=2$), K ($n=3$), Rb ($n=4$) and Cs ($n=5$) by electron impact, *J. Phys. B* **32**(10), 2323–2342 (1999), <https://doi.org/10.1088/0953-4075/32/10/303>

Sr JONO $4p^5nl'n''LSJ$ BŪSENŲ, SUŽADINANT Sr ATOMĄ ELEKTRONAIŠ, TYRIMAS

A. Kupliauskienė

Vilniaus universiteto Teorinės fizikos ir astronomijos institutas, Vilnius, Lietuva

Santrauka

Sr jono $4p^5nl'n''LSJ$ būsenos su vakansija $4p$ sluoksnyje registruojamos eksperimentuose, kuriuose sužadinamos Sr atomo būsenos su vakansija šiame sluoksnyje. Tokiuose eksperimentuose jos gali būti užpildytos trimis būdais: tiesioginės jonizacijos į $4p^5s^2\ ^2P_{1/2,3/2}$ būsenas, sužadinimo ir jonizacijos vienu metu į $4p^5nl'n''LSJ$ ($J = 1/2, 3/2$) būsenas ir suyrant Sr atomo $4p^5nl'n''LSJ$ būsenoms į Sr jono $4p^5nl'n''LSJ$ būsenas. Darbe apskaičiuoti šių procesų skerspjūviai bei Sr⁺ jono $4p^5nl'n''$ ir Sr atomo $4p^5nl'n''l''$ konfigūracijų lygmenų energijos, autojonizacijos tikimybės ir sužadinimo elektronais skerspjūviai konfigūracijų

superpozicijos metodu. Į reliatyvistines pataisas atsižvelgta ieškant radialiųjų banginių funkcijų Dirako, Foko ir Sleiterio artinyje.

Sr atomo lygmenų energijos, banginių funkcijų, transformuotų iš jjj į LSJ judesio kiekio momentų jungimo ryšį, skleidimo koeficientai panaudoti $4p^5nl'n''LSJ$ teoriniams lygmenims klasifikuoti. Didžiausi sužadinimo ir jonizacijos vienu metu bei sužadinimo ir autojonizacijos skerspjūviai, kuriems proporcingi išspinduliuotų Sr jono linijų intensyvumai, panaudoti eksperimente užregistruotoms išlėkusių elektronų 28 linijoms identifikuoti.